Journal of Building Engineering 74 (2023) 106919

Contents lists available at ScienceDirect

Journal of Building Engineering

journal homepage: www.elsevier.com/locate/jobe

Climate change and ideal thermal transmittance of residential buildings in Iran

Eugénio Rodrigues *, Nazanin Azimi Fereidani, Marco S. Fernandes, Adélio R. Gaspar

Univ of Coimbra, ADAI, Department of Mechanical Engineering, Rua Luís Reis Santos, Pólo II, 3030-788, Coimbra, Portugal

ARTICLE INFO

Keywords:
Climate change
Residential buildings
Overheating risk
Iran
Thermal transmittance

ABSTRACT

Climate change will make the Iranian climate hotter and drier. This increase in the harshness of the boundary conditions poses a new question of whether today's high-performance buildings, whose envelope thermophysical properties are optimized for the current climate, will underperform. Therefore, it is important to (i) identify the regions in Iran that will lead to such underperformance and (ii) determine to what extent the thermophysical properties will need to change to remain optimal. This paper determines and compares the ideal thermal transmittances (*U*-value) of residential building envelopes for current and future climate scenarios. The EPSAP generative design method created twelve thousand buildings with random geometries to evaluate their energy demand for heating and cooling in EnergyPlus. The *U*-values of the envelop elements for these buildings were randomly assigned and simulated for 21 locations in Iran for the current period and two future timeframes (2050 and 2080). The future weather was created using the Future Weather Generator tool to morph today's typical meteorological weather to match the EC-Earth3 data for the SSP5-8.5 scenario. The results confirm that climate change will significantly impact the energy performance of a building. However, consequences and mitigation actions will differ depending on the region. Future ideal *U*-values will be higher or lower than today's values in the center and northern regions, which are characterized by low to high heating demand in the present day. In locations with already high cooling needs, buildings will require lower, or the lowest possible, *U*-values in the future. Therefore, building professionals must incorporate climate projections in their design performance assessment. In addition, policymakers must implement building codes and guidelines that consider the anticipated impacts of climate change on building performance in different regions of the country.

1. Introduction

Energy consumption in the Iranian building sector is twice the global average [1]. If the country aims to contribute to mitigating global warming — intensified by the increasing anthropogenic carbon emissions — energy-efficient strategies in the design phase must be applied and prompted in the building sector [1]. The energy demand of buildings is among one of the few areas in this sector in which a reduction in emissions is possible [2]. In other words, an appropriate building envelope design can reduce building loads [3] and thus result in fewer greenhouse gas emissions.

Studies show that lowering the *U*-value of a building's envelope does not necessarily result in lower energy demand, and it may lead to underperformance in the current or future climate [4–6]. Thus, optimizing the building envelope's thermal transmittance for the

* Corresponding author.
E-mail address: erodrigues@uc.pt (E. Rodrigues).

https://doi.org/10.1016/j.jobe.2023.106919
Received 17 January 2023; Received in revised form 17 May 2023; Accepted 23 May 2023
Available online 24 May 2023

present and future climates is crucial. Some studies point out this need. For example, in a previous work, where the ideal *U*-values (lowest total thermal energy needs) of residential buildings in the Mediterranean region were analyzed, it was concluded that buildings in 15 out of 16 locations will have similar ideal *U*-values for the current and future climate [7].

In Podgorica, Montenegro, the energy demand of a multi-apartment building could be reduced at the end of the century by 60% [8]. Although high-insulated buildings will ensure robustness to climate change, in some regions of Italy, buildings will be prone to overheating during off-switch operating periods [9]. Nevertheless, this robustness will not always be beneficial, as buildings constructed within the legal limits will suffer from overheating over the years in the Mediterranean region, emphasizing that long-term predictive analyses have become relevant in current building design and should be considered in regulations [10]. In Morocco, summer heat gains will increase, with higher intensity in colder climate zones [11]. On the other hand, the impact of climate change on the winter months is positive due to the reduction of heat loss, which is more tangible in mild and warmer climates [11]. However, this positive impact is less significant when the buildings have lower *U*-values.

In other regions of the world, a typical office building with an optimized exterior envelope and overhangs in the present-day climate in Brisbane will remain nearly optimized in the future, while in Canberra, the same building will increase its cooling needs by up to 6% in a low-energy load context [12]. In Adelaide, building design that considers climate change must consider cooling strategies, as opposed to currently considered strategies [13]. In the case of single-family houses in 26 locations in Chile, the optimal *U*-values of walls will be higher in the future climate [14].

In the UAE, the heating and cooling demand may be reduced by up to 24% and 20%, respectively, for building envelopes with low *U*-value in Al-Ain, thus decreasing the total energy consumption by up to 16% [15]. Furthermore, for transparent elements, replacing single glazing with double glazing provides an 11% savings in cooling energy demand and between 8% and 11% savings in heating energy demand under different scenarios [15].

Studies which attempt to determine the ideal thermal transmittance of the building envelope in Iran's current and future climates are almost nonexistent [3]. Most of the studies either: (i) optimize the building envelope under the current climate, (ii) determine the impact of global warming on current buildings, or (iii) optimize the building envelope under a future scenario.

Studies carried out under the current weather conditions in Iran have shown that having the lowest *U*-value for external walls does not necessarily result in better thermal performance [1], as optimal insulation thickness depends on the wall type, orientation, and climate. By employing a life-cycle cost analysis, the optimal insulation may save up to 69% of the consumed energy [16]. Concerning transparent elements, adding nanoparticles in the insulating layer was an effective measure for reducing energy consumption [17]. Replacing air with argon gas in windows for cold climates is highly recommended, but increasing glass thickness is not cost-effective [18]. Other studies reported that the effect of wall conductivity was much higher than the glazing conductivity on building energy demands [19]. Nonetheless, an increase in wall insulation and window replacement should be prioritized in the case of budget constraints [20].

As far as the impact of climate change, overall global warming will positively impact heating-degree days and negatively influence cooling-degree days by 2075 [21]. It has also been demonstrated that most cooling needs in current days are allocated to central and eastern parts of the country (with a hot-arid climate). However, these high needs will tend to shift toward the south of Iran (with a hot-humid climate) in 2025, 2050, and 2075 [21]. In one study focusing on cities located in cold regions (located in the northwest of Iran), findings demonstrate the same behavior [22]. In a later study, when the assessment period was extended to 2100, it was concluded that there would be a delay of one month in the future yearly temperature curve and an increase of 4 °C in the average temperature for all studied locations [23]. Nonetheless, the increase in hot discomfort days will not significantly affect the energy consumption pattern [24]. In hot-humid climates, a recent study found that air-conditioning and conventional dehumidification are the only effective measures that can be applied [25]. On the other hand, indirect evaporative cooling, high thermal mass, and night ventilation are helpful strategies for buildings in hot-dry regions [25]. Under the RCP2.6 scenario, buildings with green walls and roofs might reduce heating energy consumption in Kerman (medium demand for heating) from 61% to 47% [26]. However, for Bandar Abbas, as 99% of the energy demand is for cooling, the annual energy consumption will not change by 2050 [26].

Only two recently published studies have considered the impact of climate change on optimized buildings. However, both studies merely focus on Tehran, a predominantly heating-demand city. The first study found an optimized retrofit solution for an educational building by analyzing different glazing types, insulation materials, and HVAC strategies [27]. It showed that optimized solutions for the present day were not necessarily optimal in 2080. However, the selected future optimized strategies could reduce total energy consumption by 49% for present days and 52% for the future, compared to the base case [27]. The second study, which focused on a residential building, also provided evidence that adopting energy retrofit methods, including both passive and active measures, could have a significant impact on reducing thermal discomfort and enhancing the environmental performance of the building [28]. Nevertheless, the impact of climate change on a building's external thermal loads may implicate selecting more expensive and energy-efficient cooling systems due to the projected increase in cooling demand compared to heating in the future. Despite this shift, primary energy consumption and CO_2 emissions decreased overall due to a reduction in heating demand in the examined building [28].

Based on the aforementioned literature, it was possible to conclude the following:

- There are limited studies that determine the ideal *U*-values of building envelopes in Iran's current and future climates. The studies on this topic analyzed retrofit solutions for buildings in Tehran and found that the solutions for the present day are not optimized in 2080.
- Other studies have investigated the ideal *U*-values for the current Iranian climate or analyzed the impact of climate change on current Iranian buildings. However, these topics are presented separately.

- Some studies have determined the ideal *U*-values for the future climate in other hot-arid countries. However, these may not directly apply to Iran's specific climate and building characteristics.
- The number of analyzed buildings is reduced, usually examining a single reference building. In such cases, the results may be biased as no range of performance is obtained from analyzing a large dataset, thus limiting confidence in the generalization of the findings.
- In past studies, buildings are frequently modeled as a single thermal zone, leading to incorrectly capturing the building's thermal behavior.
- In some studies, the baseline weather data and the morphing tool baseline period employ data from the last century, thus producing an unreliable comparison between current and future climates.
- Future weather data is not generated using the latest state-of-the-art climate models and IPCC's Shared Socioeconomic Pathways, which are more detailed than previous IPCC scenarios.

Therefore, to understand the impact of climate change on the built environment, buildings with ideal *U*-values under present-day and future climates must be compared, especially in a country as vast as Iran. Furthermore, as climate change does not affect all regions equally, it is also important to cover different regions of that country. Consequently, this paper will attempt to answer the following questions: "What is the impact of present-day ideal *U*-values on the energy demand of buildings in future climates?" and "What are the ideal *U*-values for the different regions of Iran under present-day and future climates?"

For this purpose, our approach has the following advantages and novelty in comparison to previous works:

- It uses 21st-century weather as a baseline (typical meteorological weather is derived from records ranging between 2004 and 2018).
- It generates future weather that matches future projections using the latest EC-Earth3 of the CMIP6 experiments. These were the basis for the latest 2022 IPCC Assessment Report.
- It studies 21 locations in Iran, covering several climate regions.
- It uses a generative design method to create 12,000 buildings with different geometries satisfying the same functional program.
- The simulation of each building is a multi-thermal zone model with detailed indoor specifications and randomly assigned envelope thermal transmittances.
- Due to the multiplicity of generated buildings and the number of locations, the analysis has a higher significance and reliability.

This paper is structured as follows: the first section presents the motivation, research gap, and research questions. An explanation as to why our approach contributes to answering the research question is also provided. Then, the materials and methods are described in detail before presenting and discussing the results in the following section. Finally, it ends by presenting the main findings and conclusions of the work.

2. Materials and methods

Fig. 1 depicts the seven steps that structure this work. The study started by selecting cities in the Iranian territory with climatic and geographic diversity (step 1). Then, 21st-century weather was retrieved, and the integrity was checked. This data was used as the present-day climate and mathematically transformed into the future climate in the third step. In the fourth step, random geometries of single-family houses were created using a generative design method. When simulating each building for each location, thermal transmittances were randomly assigned to each of the envelope's opaque and transparent elements. In the fifth step, the energy demand for heating and cooling in all of the buildings was stored for all scenarios. In the sixth step, a preliminary analysis was carried out to group locations according to the future ideal *U*-values. Lastly, datasets were statistically analyzed, and findings were synthesized.

2.1. Selection of locations

Iran has highly diverse climatic conditions as the country spans a wide range of latitudes, has different terrain altitudes, and is also proximate to water bodies [22]. Also, the country is in southwest Asia, and the subtropical aridity of the Arabian Desert and the subtropical humidity of the eastern Mediterranean area influences its climate. In addition, Iran hosts two major mountain ranges,

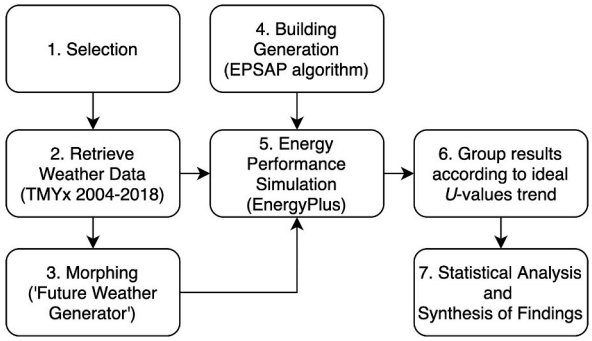

Fig. 1. Study concept framework.

namely Alborz in the north and Zagros in the west. These mountain ranges block humidity and prevents clouds from reaching the central and southeastern parts of the country, including the Eurasian Plate [25].

Relatively to temperature distribution, Iran's temperature increases as you travel from the north to the south and from the west

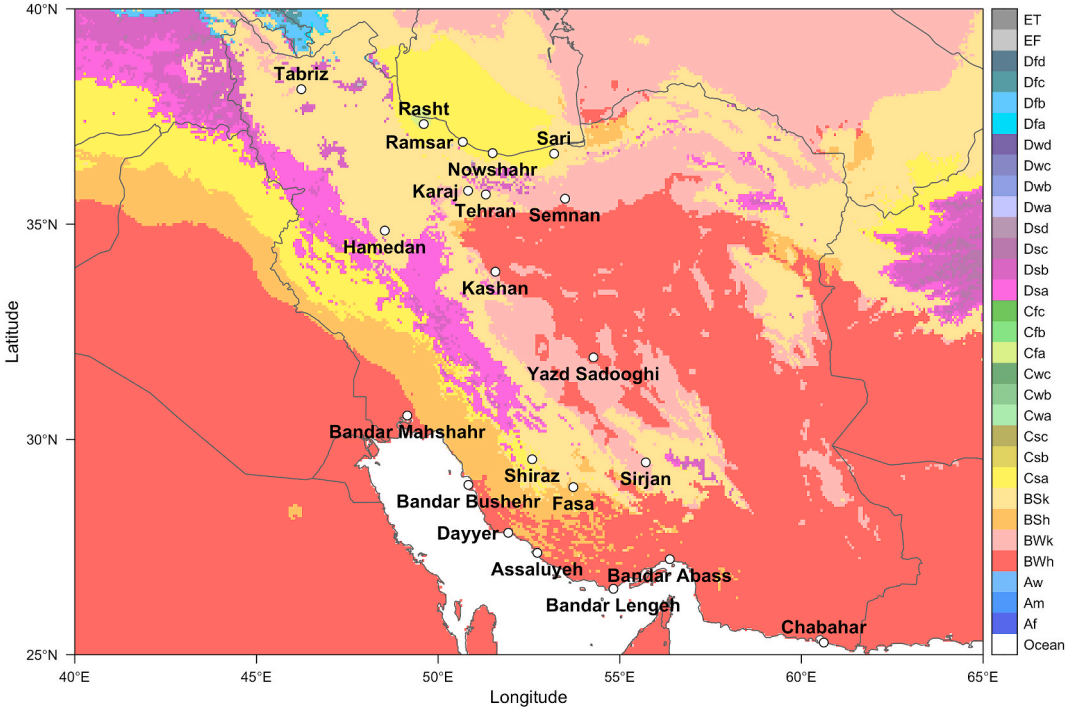

(a) Present-day climate.

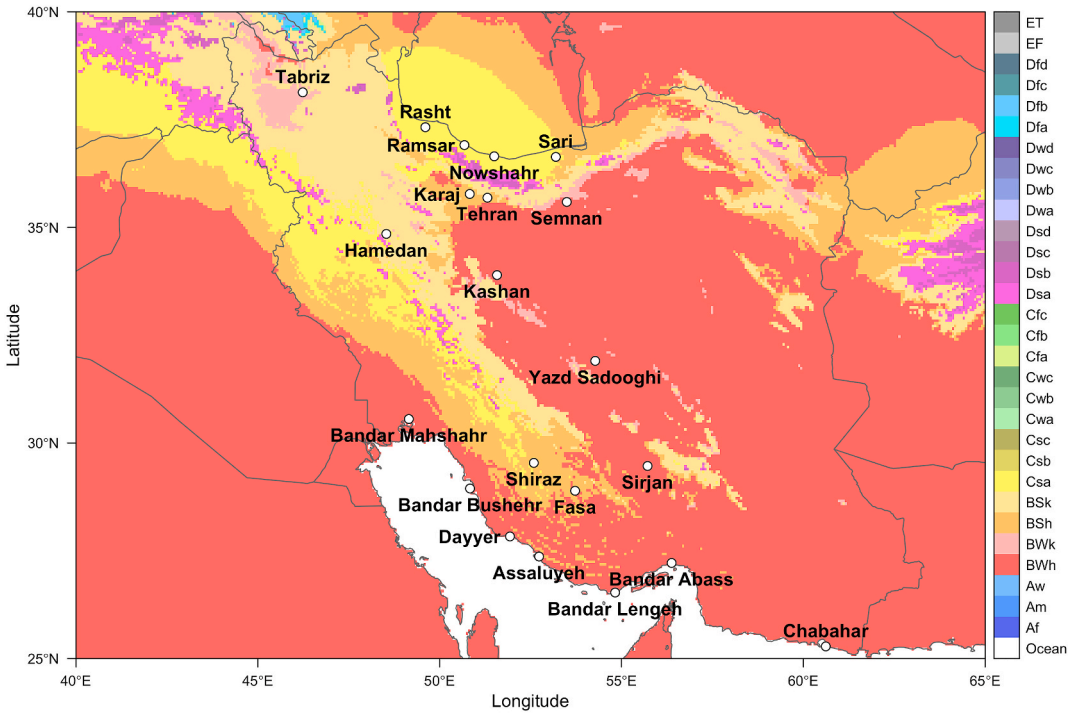

(b) Future climate (RCP8.5, 2071-2100).

Fig. 2. Maps depicting current and future climate classifications (produced from data available in Ref. [29]).

towards the east. The highest values are found in the southern regions, and the lowest temperatures are in the north. The country has a semi-dry climate, except for the wet zone in the southern coastal plains of the Caspian Sea and the relatively wet areas in the west [25].

As stated in the literature review, climate change may affect each specific climate region differently; therefore, in order to cover all climates regions in Iran and analyze the ideal *U*-values for each specific climate region, the following criteria were used to select locations in Iran: (i) they cover all climate types in Iran according to Köppen-Geiger climate classification [29], (ii) they are distributed spatially over Iran's latitudes with predominance in populated and geographically diverse regions, (iii) the hourly weather data is freely available, and (iv) the historical meteorological data matches the period of the weather morphing tool used.

In total, twenty-one locations were selected. These include cities on the coast of the Caspian Sea (Rasht, Ramsar, Nowshahr, and Sari), the coast of the Persian Gulf (Bandar Mahshahr, Bandar Bushehr, Dayyer, Assaluyeh, Bandar Abaass, Bandar Lengeh, and Chabahar), and in the interior (Tabriz, Karaj, Hamedan, Tehran, Semnan, Kashan, Yazd Sadooghi, Shiraz, Sirjan, and Fasa). Fig. 2 displays two 1-km resolution maps with Köppen-Geiger climate classification created from the data provided by Beck et al. [29] for the present-day (1980–2016) and the future scenario (2071–2100, RCP8.5). These were derived from an ensemble of 32 climate model projections. These locations cover all possible current climate types in Iran, including BWh (Arid, desert, hot), BSh (Arid, steppe, hot), BWk (Arid, desert, cold), BSk (Arid, steppe, cold), Csa (Hot-summer Mediterranean climate), Cfa (Humid subtropical climate), and Dsa (humid continental climate). At first glance, Iran will be hotter and drier in the future. Thus, the BWh is the climate type that covers the largest area of the territory.

Table 2 provides more in-depth details on the geographical and climatic information of the selected locations for both timeframes. The climate classifications will change for nine locations until the end of the century: Tabriz, Rasht, Sari, Karaj, Tehran, Semnan, Sirjan, Fasa, and Bushehr. Overall, all cities will experience warmer summers and dryer seasons.

2.2. Weather morphing

Future weather data was obtained by statistically transforming present-day weather data to match the projected scenario from a climate model. The procedure is essentially a delta method and thus does not require bias correction. In this study, the data was morphed using the Future Weather Generator [30]. The tool was developed using data from one of the latest climate models, and it addresses several issues found in other weather morphing tools. The climate data originated from the EC-Earh3 [31] general circulation model and was used in the CMIP6 experiments (the basis for the 2022 IPCC's 6th Assessment Report). The EC-Earth3 climate system comprises various physical domains and system components that capture the atmosphere, ocean, sea ice, land surface, dynamic vegetation, atmospheric composition, ocean biogeochemistry, and the Greenland Ice Sheet [31]. In the standard configuration, the land and atmosphere domains are covered by HTESSEL and IFS, respectively, while the ocean ice is modeled with NEMO3.6 and the sea ice by LIM3. These domains and components are coupled using the OASIS3-MCT coupler. The EC-Earth3 grid has an 80 km atmospheric resolution (T255L91) and a 1.0° ocean resolution (ORCA1L75). The validation of EC-Earth3 can be found in Refs. [32,33].

This study used the Shared Socioeconomic Pathways SSP5-8.5, which projects that current CO_2 emissions will roughly double by 2050 and the average global temperature will rise by 4.3 °C in 2100. Although not the most plausible scenario, the SSP5-8.5 will be the most impactful; therefore, several researchers consider its study important [34]. Monthly changes from the current climate and the SSP5-8.5 scenario are computed from each median month of the present-day period (1985–2014) and the two future timeframes—2050 (2036–2065) and 2080 (2066–2095). The tool includes a world grid with 131,072 points, and the monthly changes for the variables are spatially downscaled using a bilinear interpolation method of the four nearest points of the grid to the weather data's location. Information on the tool and the method formulation may be found on the tool's website [35].

2.3. Building geometry generation

The building geometries were created using the EPSAP algorithm [36], a generative design method. EPSAP is a population-based hybrid evolution strategy that substitutes the traditional mutation and crossover operators with a stochastic hill climbing method that carries out different geometric and topologic transformations to every candidate design in the population. Such transformations comprise the translation, reflection, rotation, stretching, and alignment of a single space to a cluster of spaces. If these transformations produce an improved solution, the change is kept. The algorithm determines if the transformation leads to an improved solution by minimizing a weighted-sum cost function of seventeen penalty functions. These penalty functions evaluate (i) the building's maximum gross and construction areas, compactness, and circulation areas, (ii) the overflow, connectivity, overlapping, fixed position, minimum dimensions, and relative importance of the zones, and (iii) the accessibility, minimum dimensions, overlapping, orientation, and fixed position of the openings. Further methodological detail on this algorithm may be found in Refs. [37,38] and its validation in Ref. [39].

As a result, the algorithm creates alternative designs by arranging the indoor spaces of a given functional program. The building designs satisfy the minimum and maximum dimensional specifications for rooms, windows, and doors, as well as topological specifications, such as relations between rooms and elements orientations. In other words, buildings may differ in volume, floor area, window-to-wall ratio, orientation, compactness, and indoor arrangement, among other aspects, but all will have the same functional program—*e.g.*, an apartment having two bedrooms, a kitchen, a bathroom, and a living room.

The functional program for this study corresponded to a two-story single-family house used in previous work [7]. The rooms are distributed on two floors, served by a staircase. A hall, a living room, a kitchen, and a bathroom are on the ground floor. On the second floor, a corridor connects three bedrooms and a second bathroom. The algorithm will allocate rooms with the smallest side greater than 1.8 m for the kitchen, 3.2 m for the living room, 2.2 m for the bathrooms, and 2.7 m for the bedrooms. The exterior doors will have a 1 m width by 2 m height. The exterior windows will have a 1.8 m width by 1 m height in the double bedrooms and a 2.8 m width by 2 m height in the living room. In the kitchen and the single bedroom, the windows will have 1.2 m by 1 m. The bathroom on the ground floor will have a 0.6 m-squared window. All the interior doors will measure at least 0.9 m by 2 m.

Fig. 3 illustrates 24 samples of building geometries from the dataset. Twelve thousand geometries were generated with different volumes, orientations, and floor plan arrangements.

2.4. Building performance simulation

The energy performance of each building in the dataset was calculated using EnergyPlus in a multi-zone annual simulation. EnergyPlus is coupled to the EPSAP algorithm and runs at the end of the building generation process [40]. The selected time step for each simulation is 15 min, and the outputs are related to the thermal energy demand of the building—*i.e.*, total energy, heating, and cooling needs. The internal gains, HVAC, airflow, and construction specifications are described in the following sections.

2.4.1. Internal gains specifications

The internal gains correspond to a typical single-family house of five occupants. The lighting and equipment design levels and schedules are based on the building's zone type and occupancy. The living room has an activity level of 110 W·person^{-1}, the bathrooms 207 W·person^{-1}, the kitchen 190 W·person^{-1}, and the bedrooms 72 W·person^{-1}. Relatively to the electric equipment, the kitchen has a design level of 1440 W, bedrooms 250 W, living room 350 W, and bathrooms 100 W. The electric lighting level is 7.5 W m^{-2} in the living room, bathrooms, and bedrooms, while in the kitchen, it is 5 W m^{-2}. Daylighting control dims the light intensity in the zones with exterior windows and turns the artificial light off when sunlight exceeds 300 lux. The window shadings are closed during nighttime. See Ref. [7] for additional details.

2.4.2. HVAC and airflow specifications

This study also follows the HVAC and airflow specifications in Ref. [7]. The living room and the bedrooms are the only rooms with heating and cooling, with the system's availability depending on the occupancy in each room. The HVAC template zone ideal loads air system is used, and the temperature thermostat setpoints for cooling and heating are 25 °C and 20 °C, respectively, according to the Iranian Building Code.

Mechanical ventilation is also considered in the kitchen and bathrooms, with a 0.6 h^{-1} air change exhaust rate occurring during occupancy defined for these zones. Additional 0.2 h^{-1} and 0.1 h^{-1} air changes are considered for the outdoor air infiltration in zones with and without exterior openings, respectively.

2.4.3. Construction specifications

The elements with varying thermal transmittances are the exterior walls, roofs, suspended floors, and windows. The thermal mass of these elements is equivalent to that of the interior slab and the element's surface area. The *U*-value of the opaque elements is randomly assigned before simulating the energy demand, and the values vary between 0.05 W m^{-2} K^{-1} and 1.25 W m^{-2} K^{-1} in steps of 0.05 W m^{-2} K^{-1}. The *U*-value should be understood as the thermal transmittance of the whole opaque envelope. Regarding exterior windows, the *U*-value is proportionally paired with one of the opaque elements and varies from 0.2 W m^{-2} K^{-1} to 5.0 W m^{-2} K^{-1} in steps of 0.2 W m^{-2} K^{-1}. The pairing of *U*-values follows the tendency of real cases, where the *U*-values of both opaque and transparent elements decrease or increase proportionally. Each pair of *U*-values has, on average, 480 buildings. Solar absorptance of 0.75 was used for all outer surfaces. Although the solar heat gain coefficient also tends to vary according to the window *U*-value, a fixed 0.6 was chosen to capture only the impact of thermal transmittance variation. A visible transmittance of 0.6 was used. The thermophysical properties of the construction elements are presented in Table 1 for the fixed (interior elements) and random construction (exterior

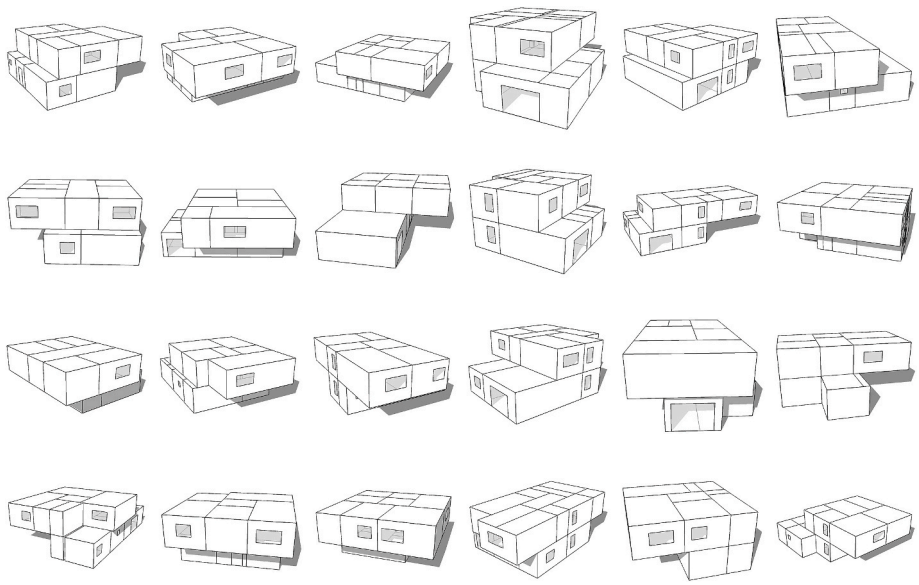

Fig. 3. Examples of the 12,000 generated building geometries.

elements). The buildings are considered to have high thermal mass.

2.5. Comparison analysis and synthesis

A dataset of the buildings' geometry, construction, and performance data was created for each location with the present-day, 2050, and 2080 timeframes. For the comparison analysis, the locations were grouped according to the trend of the ideal *U*-value over time. Then, for each group, the statistical analysis was conducted by splitting each dataset into groups according to the thermal transmittance values of their envelope elements (25 pairs of *U*-values for opaque and transparent elements). Next, the average total energy demand for heating and cooling, the standard deviation, and the differences in average total energy, cooling, and heating needs were calculated between the present-day and the 2050 and 2080 timeframes. The pair of *U*-values that produce the lowest average total energy needs is the ideal *U*-values for that location—optimum values for a set of buildings. Knowing the ideal *U*-values for the present-day and future timeframes makes it possible to estimate the trend of ideal thermal transmittance values through time and the risk that global warming poses in buildings overheating.

3. Results and discussion

For present-day climate, 21st-century hourly weather for each location was retrieved from the climate.onebuilding.org website [41]. The weather data follows the TMY/ISO 15927–4:2005 and is derived from meteorological records between 2004 and 2018. Table 3 presents the most relevant weather variables for buildings' energy performance. This table includes the variables for the present-day weather as well as weather for the 2050 and 2080 timeframes after morphing the former to match the SSP5-8.5 scenario. The changes in the variables align with the characteristics of the climate classification map for the future presented in Fig. 2b above. For example, the average dry bulb temperature may increase to 4.6 °C in 2050 and 7.9 °C in 2080. These changes demonstrate that Iran will be particularly impacted by global warming, showing average temperatures greater than the global average temperature of 4.4 °C predicted for the SSP5-8.5 scenario in 2100. Also, daily minimum and maximum average temperatures will increase for all locations, thus reducing the night cooling potential. Regarding relative humidity, the difference between the present-day and 2050 ranges show a decrease, except for Ramsar and Yazd. The trend varies from a negligible −0.06% to −5.5% for 2050 and -1% to −10.1% for 2080. As for global horizontal radiation, the differences range from −2.13 W h m^{-2} to −4.21 W h m^{-2} in 2050 and from −0.96 W h m^{-2} to

Table 1
Thermophysical properties of the building elements. Based on Ref. [7].

Element	Layer	Thick. (m)	k ($W{\cdot}m^{-1}{\cdot}K^{-1}$)	ρ ($kg{\cdot}m^{-3}$)	c_p ($J{\cdot}kg^{-1}{\cdot}K^{-1}$)	U ($W{\cdot}m^{-2}{\cdot}K^{-1}$)	Mass ($kg{\cdot}m^{-2}$)	α(−)	SHGC (−)	VT (−)
Ground floor	Structural layer	0.200	1.730	2245.6	836.8	0.437	509.69	–	–	–
	Insulation layer	0.080	0.040	32.1	836.8					
	Filling layer	0.020	0.800	1600.0	840.0					
	Regulation layer	0.010	0.220	950.0	840.0					
	Finishing layer	0.020	0.200	825.0	2385.0					
Interior door	Finishing layer	0.005	0.200	825.0	2385.0	2.009	21.15	–	–	–
	Structural layer	0.030	0.067	430.0	1260.0					
	Finishing layer	0.005	0.200	825.0	2385.0					
Interior wall	Finishing layer	0.020	0.220	950.0	840.0	4.499	195.01	–	–	–
	Structural layer	0.070	1.730	2243.0	836.8					
	Finishing layer	0.020	0.220	950.0	840.0					
Interior slab	Finishing layer	0.020	0.220	950.0	840.0	2.841	494.12	–	–	–
	Structural layer	0.200	1.730	2245.6	836.8					
	Regulation layer	0.010	0.220	950.0	840.0					
	Finishing layer	0.020	0.200	825.0	2385.0					
Opaque (exterior wall, roof, and suspended floor)	Thermal mass is equivalent to the mass of the interior slab.					RAND {0.05, …, 1.25}	–	0.75	–	–
Transparent (window)	–					RAND {0.2, …, 5.0}	–	–	0.6	0.6

k – thermal conductivity, ρ – density, c_p – specific heat, U – thermal transmittance, α – solar absorptance, SHGC – solar heat gain coefficient, VT – visible transmittance.

Table 2
Geographic data and climate classification (sorted in descending latitude) [29]. Future climate classification that differs from the present-day climate classification is marked in bold.

Location				Climate		
City	Lat.	Long.	Alt. (m)	Present-day	Present-day description	Future[a]
Tabriz	38.13° N	46.23° E	1359	BSk	Arid, steppe, cold	**BWk**
Rasht (coastal)	37.32° N	49.60° E	−12	Cfa	Temperate, no dry season, hot summer	**Csa**
Ramsar (coastal)	36.91° N	50.68° E	−21	Csa	Temperate, dry summer, hot summer	Csa
Nowshahr (coastal)	36.65° N	51.50° E	−21	Csa	Temperate, dry summer, hot summer	Csa
Sari (coastal)	36.63° N	53.19° E	10	BSh	Arid, steppe, hot	**Csa**
Karaj	35.77° N	50.82° E	1271	BSk	Arid, steppe, cold	**BSh**
Hamedan	34.85° N	48.53° E	1749	BSk	Arid, steppe, cold	BSk
Tehran	35.68° N	51.31° E	1207	BSk	Arid, steppe, cold	**BSh**
Semnan	35.59° N	53.49° E	1117	BWk	Arid, desert, cold	**BWh**
Kashan	33.89° N	51.57° E	1056	BWh	Arid, desert, hot	BWh
Yazd Sadooghi	31.90° N	54.27° E	1235	BWh	Arid, desert, hot	BWh
Shiraz	29.53° N	52.58° E	1499	BSh	Arid, steppe, hot	BSh
Sirjan	29.46° N	55.71° E	1739	BSk	Arid, steppe, cold	**BWh**
Fasa	28.89° N	53.72° E	1298	BSh	Arid, steppe, hot	**BWh**
Bandar Mahshahr (coastal)	30.55° N	49.15° E	2	BWh	Arid, desert, hot	BWh
Bandar Bushehr (coastal)	28.94° N	50.83° E	20	BSh	Arid, steppe, hot	**BWh**
Dayyer (coastal)	27.83° N	51.93° E	4	BWh	Arid, desert, hot	BWh
Assaluyeh (coastal)	27.36° N	52.73° E	8	BWh	Arid, desert, hot	BWh
Bandar Abass (coastal)	27.21° N	56.37° E	6	BWh	Arid, desert, hot	BWh
Bandar Lengeh (coastal)	26.53° N	54.82° E	20	BWh	Arid, desert, hot	BWh
Chabahar (coastal)	25.28° N	60.61° E	8	BWh	Arid, desert, hot	BWh

[a] Projected climate classification under scenario RCP8.5 and timeframe 2071–2100 [29].

−3.37 W h m^{-2} in 2080, showing a slight decrease. Today's wind speed will be similar to the ones in future timeframes.

From an initial assessment of findings, cities were grouped based on the trend of ideal *U*-values in order to discuss and analyze the results in a more organized format: Group 1 – locations where buildings will require higher values in the future, Group 2 – lower or equal values in the future, and Group 3 – where values should be the lowest possible for the present day and the future. Fig. 4 depicts the geographical distribution of the three groups in Iran. It is possible to observe that Group 1 is spread across the north of the country and along the coast of the Caspian Sea, Group 2 is concentrated in the interior, while Group 3 is located more along the coast of the Persian Gulf.

Figs. 5–7 show the results of simulations for 12,000 buildings in 21 locations in Iran for all timeframes. The energy performance of the buildings of each of the 25 pairs of *U*-values for opaque and transparent elements was averaged (*x*-axes; the top line corresponds to the *U*-values for transparent elements and the bottom line to the *U*-values for opaque elements). A total number of 756,000 simulations were conducted. Fig. 5 depicts the results for Group 1, Fig. 6 for Group 2, and Fig. 7 for Group 3.

In these three figures, the first column on the left presents the average total energy demand for buildings for the present-day, 2050, and 2080 in green, orange, and red lines, respectively. Additionally, the cooling energy demand for each timeframe is depicted by the continuous blue line. The heating demand is easily perceived by the difference to the total energy demand. Also, for each timeframe, the small black circumference represents the ideal pair of *U*-values (lowest energy use for heating and cooling). The graphs in the second column plot the standard deviation of the total energy demand (σ energy). The third column displays the difference between total energy needs (Δ energy) for the present-day and 2050 timeframes. Finally, the graphs in the last column represent the difference in cooling (blue bars) and heating (red bars) energy demands (Δ energy) between the present-day and the 2050 timespan. The highest and the lowest relative differences (%) are also displayed in the graphs.

Fig. 5 depicts the results for the locations from Group 1. According to the Building Code of Iran [42], these locations are characterized by low to high heating needs in the present-day climate. However, as depicted by the graphs in the first column, the energy demand for buildings is mainly for cooling when the ideal *U*-values (depicted by the blue line) are reached. As the thermal transmittance decreases until the ideal values are reached, the heating demand also decreases significantly, and the cooling needs slightly increase in the present-day climate. This finding indicates that the thermal transmittance values for today's buildings may be lowered.

When comparing the energy performance curves between present-day and future climates, total energy demand is greater today for high *U*-values in Tabriz, Karaj, and Hamedan. This difference is directly related to the location of these three cities, which is in the interior of northern Iran with altitudes above 1000 m, while the remaining locations in Group 1 are on the coast of the Caspian Sea. The worse energy performance in the present-day climate for the highland cities ranging from medium to high *U*-values shows buildings with high heating demand. However, the heating needs will substantially decrease when the outside air temperature increases. Therefore, although cooling needs will increase, the energy balance benefits buildings with high *U*-values in a warmer future (see last column). As shown by the differences in total energy in the third column, the impact of the reduction of heating demand is such that it causes overall energy demand to be −12% for Tabriz, −8% for Karaj, and −20% for Hamedan in 2050.

However, Group 1 buildings located along the coast of the Caspian Sea will require more energy for air conditioning in 2050 than in the present day across the whole *U*-value range, and the same is true when comparing 2050 to 2080. The higher total energy demand in the future results from significantly higher cooling demand, despite the reduction in heating demand (see last column). As observed in

Table 3
Dry-bulb temperature, relative humidity, global horizontal radiation, and wind speed variables comparison between present-day and 2050 and 2080 timeframes (hourly average and present-day to timeframe difference).

Location	Timeframe	Dry-bulb temperature				Relative humidity		Global horizontal radiation		Wind speed	
		°C	Δ °C	Min °C	Max °C	%	Δ %	W·h·m^{-2}	Δ W·h·m^{-2}	m·s^{-1}	Δ m·s^{-1}
Tabriz	Present-day	13.5		8.2	19.3	51.4		205.2		3.7	
	2050	18.0	4.4	12.4	24.0	45.9	−5.5	203.1	−2.1	3.7	0
	2080	21.3	7.8	15.7	27.3	41.3	−10.1	203.1	−2.2	3.8	0.1
Rasht (coastal)	Present-day	16.7		12.9	20.9	83.3		165.5		1.8	
	2050	19.5	2.8	15.7	23.7	82.4	−0.9	161.5	−4.0	1.7	−0.1
	2080	21.9	5.2	18.0	26.1	80.5	−2.8	162.2	−3.3	1.7	−0.1
Ramsar (coastal)	Present-day	17.2		14.3	20.1	81.2		169.3		2.0	
	2050	19.9	2.7	17.0	22.7	81.9	0.8	165.3	−3.9	1.9	−0.1
	2080	22.2	5.0	19.2	25.1	81.3	0.1	166.0	−3.3	1.9	−0.1
Nowshahr (coastal)	Present-day	17.1		13.8	20.3	81.9		167.9		2.2	
	2050	20.0	2.9	16.7	23.3	77.7	−4.1	163.7	−4.2	2.1	−0.1
	2080	22.5	5.5	19.1	25.9	74.1	−7.8	164.5	−3.4	2.1	−0.1
Sari (coastal)	Present-day	17.3		12.8	22.2	79.0		176.8		2.8	
	2050	20.1	2.9	15.6	25.0	77.1	−1.9	172.7	−4.1	2.7	−0.1
	2080	22.6	5.3	18.0	27.5	74.7	−4.3	173.4	−3.4	2.7	−0.1
Karaj	Present-day	14.2		6.8	22.0	41.8		215.5		4.2	
	2050	17.9	3.7	10.6	25.8	40.4	−1.3	212.6	−2.9	4.2	0
	2080	21.1	6.9	13.6	29.2	37.4	−4.4	214.4	−1.0	4.2	0
Hamedan	Present-day	12.6		4.9	19.9	46.4		220.3		2.5	
	2050	17.1	4.6	9.1	24.8	41.2	−5.3	217.9	−2.4	2.5	0.1
	2080	20.4	7.9	12.4	28.1	37.4	−9.0	217.9	−2.4	2.6	0.1
Tehran	Present-day	18.7		13.7	23.3	35.3		215.8		3.1	
	2050	22.3	3.6	17.3	26.9	34.0	−1.3	212.7	−3.1	3.1	0
	2080	25.5	6.8	20.4	30.2	31.3	−4.0	214.7	−1.1	3.1	0
Semnan	Present-day	18.9		13.4	24.1	33.2		224.0		2.1	
	2050	22.6	3.7	17.2	27.8	31.7	−1.5	221.0	−3.0	2.1	0
	2080	25.9	7.0	20.3	31.2	28.9	−4.3	222.8	−1.2	2.1	0
Kashan	Present-day	19.6		13.0	26.1	37.4		232.4		1.3	
	2050	23.2	3.6	16.6	29.7	35.8	−1.6	229.3	−3.1	1.3	0
	2080	26.4	6.8	19.6	33.0	33.0	−4.5	231.4	−1.0	1.3	0
Yazd Sadooghi	Present-day	20.6		13.9	27.0	25.4		238.1		2.7	
	2050	24.3	3.7	17.5	30.7	25.6	0.2	235.2	−3.0	2.7	0
	2080	27.5	6.8	20.5	34.0	24.3	−1.1	237.2	−1.0	2.7	0
Shiraz	Present-day	18.9		10.4	26.1	38.1		243.0		1.7	
	2050	22.6	3.6	14.0	29.8	36.0	−2.1	240.0	−3.0	1.7	0
	2080	25.7	6.8	17.0	33.1	33.0	−5.1	242.1	−1.0	1.7	0
Sirjan	Present-day	18.2		10.9	25.1	32.4		254.8		3.1	
	2050	21.8	3.7	14.5	28.8	31.7	−0.7	251.9	−3.0	3.1	0
	2080	25.0	6.8	17.5	32.0	29.5	−2.9	253.9	−1.0	3.1	0
Fasa	Present-day	19.9		11.1	28.4	37.3		251.4		1.8	
	2050	23.6	3.7	14.7	32.1	35.3	−2.0	248.4	−3.0	1.8	0
	2080	26.7	6.8	17.7	35.4	32.4	−4.9	250.4	−1.0	1.8	0
Bandar Mahshahr (coastal)	Present-day	26.2		19.5	33.1	46.4		239.1		3.8	
	2050	29.1	2.8	22.3	35.9	46.3	−0.1	235.1	−4.1	3.6	−0.2
	2080	31.5	5.2	24.7	38.4	45.4	−1.0	235.8	−3.4	3.6	−0.2
Bandar Bushehr (coastal)	Present-day	25.9		21.7	29.7	60.5		238.8		3.1	
	2050	28.7	2.8	24.5	32.5	58.2	−2.3	234.8	−4.0	2.9	−0.1
	2080	31.1	5.2	26.9	34.9	55.9	−4.7	235.4	−3.4	2.9	−0.1
Dayyer (coastal)	Present-day	27.6		23.6	31.3	54.2		247.3		3.2	
	2050	30.4	2.8	26.5	34.1	52.2	−2.0	243.3	−4.1	3.1	−0.2
	2080	32.8	5.2	28.8	36.6	50.2	−3.9	244.1	−3.3	3.1	−0.2
Assaluyeh (coastal)	Present-day	26.5		20.4	33.0	61.2		247.3		2.9	
	2050	29.3	2.8	23.2	35.8	58.6	−2.6	243.2	−4.1	2.8	−0.1
	2080	31.7	5.2	25.6	38.3	56.3	−4.9	244.0	−3.3	2.7	−0.1
Bandar Abass (coastal)	Present-day	27.5		22.6	32.4	64.6		246.1		3.7	
	2050	30.3	2.8	25.4	35.2	61.4	−3.2	242.1	−4.1	3.5	−0.2
	2080	32.7	5.2	27.7	37.7	58.6	−6.0	242.8	−3.3	3.5	−0.2
Bandar Lengeh (coastal)	Present-day	27.3		23.5	31.3	62.9		252.2		3.8	
	2050	30.1	2.8	26.3	34.1	59.7	−3.2	248.1	−4.1	3.7	−0.2
	2080	32.5	5.2	28.6	36.6	57.0	−5.9	248.9	−3.3	3.7	−0.2
Chabahar (coastal)	Present-day	26.7		23.1	30.6	68.2		237.5		2.7	
	2050	29.5	2.8	25.9	33.4	64.5	−3.7	233.4	−4.1	2.6	−0.1
	2080	31.9	5.2	28.2	35.8	61.5	−6.7	234.1	−3.3	2.6	−0.1

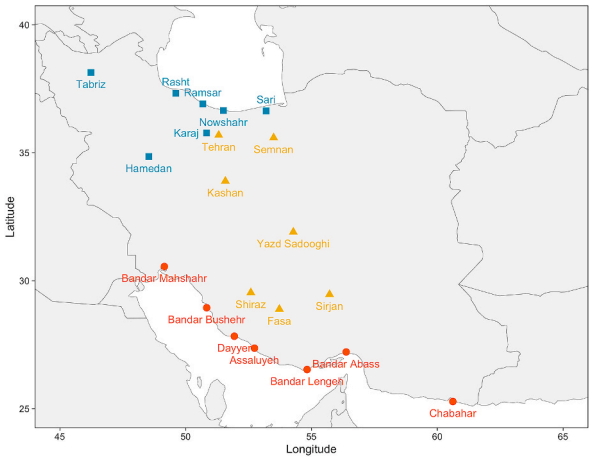

Fig. 4. Locations grouped by the trend of the ideal *U*-values. Blue squares depict Group 1, yellow triangles Group 2, and red dots Group 3. (For interpretation of the references to colour in this figure legend, the reader is referred to the Web version of this article.)

the third column, the increase in total energy demand is not the same across the range of *U*-values. Energy demand for buildings may increase up to 8% for high *U*-values and 31% for low *U*-values.

For all locations in this group, the future ideal *U*-values will be higher than the present-day ideal *U*-values (marked with a black circumference in the first column). The difference between the future and the present-day ideal *U*-values is minimal for coastal cities across the Caspian Sea. However, for cities in the highlands, the differences are greater.

Table 4 presents the energy performance of present-day ideal *U*-values in future timeframes. The results show that for cities in higher altitudes, which are also located in the interior, buildings with ideal *U*-values in the current climate will consume more energy in 2050 and 2080 compared to the ideal future U-value for each timeframe—*e.g.*, in 2080, Tabriz shows a difference of 2.8%, Karaj 3.8%, and Hamedan 7.6%. However, coastal locations present relatively small energy differences—lower or equal to 1.4% in 2050 and approximately 1% in 2080—and smaller thermal transmittance variations.

The reason why the ideal *U*-values increase (even if slightly) in 2050 and 2080 may be found in the delicate balance between outdoor air temperatures and the capacity of the buildings to release heat. This also explains why buildings with current optimum thermal transmittance values will overheat in the future. As shown in Table 3, the average temperatures for locations in the highlands will rise by 4 °C and 8 °C in 2050 and 2080, respectively. This steady rise in average temperature will result in outdoor temperatures falling within the air conditioning setpoints in 2080. Therefore, buildings' interior gains will have a detrimental impact on indoor thermal performance, resulting in the need for heat release, which is attained through lower thermal resistance of the envelope elements. A similar effect is observed for the remaining locations in Group 1, but with lesser impact (thus the smaller difference in current and future ideal *U*-values). In these cases, the outdoor temperatures do not increase as much (less than 3 °C and 6 °C in 2050 and 2080, respectively), meaning that only a small rise in thermal transmittance is needed.

Fig. 6 presents the results for Group 2, locations in the central plateau of Iran, namely Tehran, Semnan, Kashan, Yazd Sadooghi, Shiraz, Sirjan, and Fasa. The graphs from the first column show that total energy demand and cooling demand (continuous blue lines) will increase in the future timeframes (2050, 2080) for all locations across the *U*-value range. The relative increase in energy demand may reach 23% for buildings with low *U*-values and 11% for high *U*-values in the 2050 timeframe. According to Iran's Building Code [42], buildings in these locations have medium heating needs in the present-day climate. However, those needs are minimal today if the ideal *U*-values are used, as shown in Fig. 6.

While locations in Group 1, particularly cities in the interior and highlands, are characterized by a major decrease in heating needs, Group 2 displays a lesser reduction. As a result, the increase in cooling demand (blue bars) is greater than the reduction in heating demand (red bars) on the overall energy demand of buildings in these locations; thus, the present-day values (last column) never have higher energy demands than for 2050.

Relatively to future ideal *U*-values, all locations in 2050 will require the same values as for the present-day, with the exception of Semnan, which shows an increment in 2050. Nonetheless, when comparing 2080 to the present day, all locations will need lower ideal *U*-values except for Sirjan, which displays the same ideal thermal transmittance values.

In the case of Semnan, the ideal *U*-values will increase slightly, as opposed to the other locations in Group 2 for 2050. However, this location has been included in the group since it follows the same trend in 2080. The energy demand difference between present-day and future ideal *U*-values is minimal in 2050, meaning that building geometry plays a higher role.

As shown in Table 5, present-day ideal *U*-values will still be effective in 2050 for all cities except for Semnan, where the difference in energy demand will be lower than 1%. However, for 2080, all locations require lower ideal *U*-values than in the present day, except for Sirjan. Among those, Yazd Sadooghi and Fasa have the highest energy differences (up to 3.7%) and the highest ideal thermal transmittance variations for the 2080 timeframe. Yazd Sadooghi will have decrements of 0.15 W m^{-2} K^{-1} and 0.6 W m^{-2} K^{-1} for opaque and transparent elements, respectively, and Fasa 0.2 W m^{-2} K^{-1} and 0.8 W m^{-2} K^{-1}.

The cases of Yazd Sadooghi and Fasa are particularly interesting because they start showing the trend found in Group 3. In 2080,

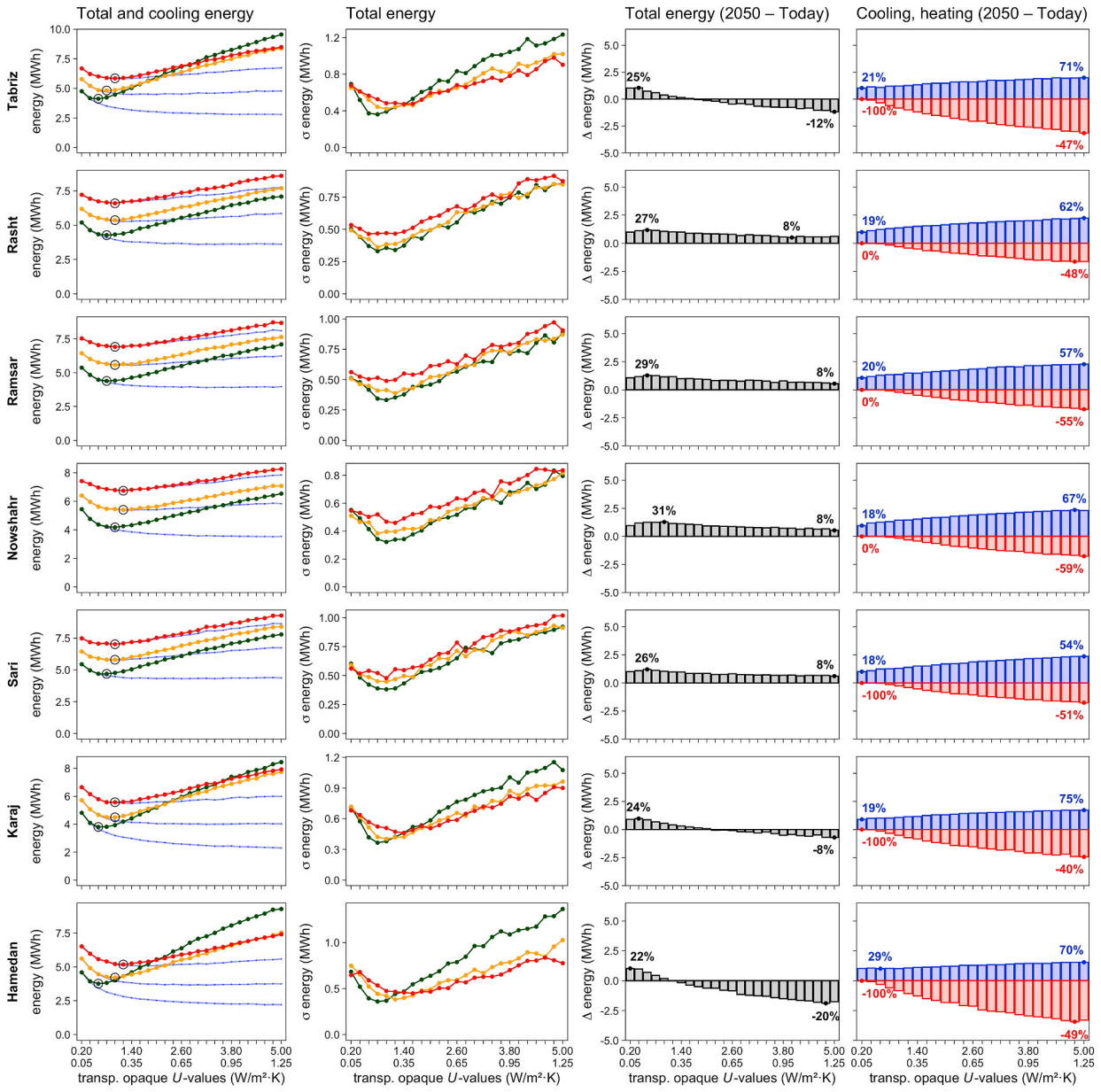

Fig. 5. Group 1– Comparison between present-day (green lines), 2050 (orange), and 2080 (red) timeframes. Graphs in the first column depict the average total energy needs – blue lines illustrate the cooling energy needs, and black circles indicate the ideal pair of *U*-values for each timeframe. The second column presents the standard deviation (σ). The third and fourth columns present the difference in total energy needs (Δ) and cooling (blue bars) and heating (red bars) energy needs (Δ) between the 2050 and present-day timeframes. (For interpretation of the references to colour in this figure legend, the reader is referred to the Web version of this article.)

these locations are almost only characterized by having cooling needs due to outdoor temperatures being so high the whole year that the ideal *U*-values must be the lowest possible to prevent heat gains through the building envelope. Table 3 above shows that both those cities have average temperatures near 27 °C in 2080 and daily minimum average temperatures above 18 °C, which is almost the heating setpoint.

As stated, the trend seen in Yazd Sadooghi and Fasa is observed in all timeframes for Group 3. This group includes locations in the south of Iran, which are adjacent to the Persian Gulf, whose climatic conditions are heavily influenced by this body of water [24]. The locations are Bandar Mahshahr, Bandar Bushehr, Dayyer, Assaluyeh, Bandar Abbas, Bandar Lengeh, and Chabahr.

According to the Iranian Building Code [42], buildings in these locations present high cooling needs for the present-day climate. This performance characteristic is in line with what is observed in Fig. 7, showing an overlap between cooling needs and total energy demand, depicted by graphs in the first column.

Since the only demand is cooling, as global warming continues to settle in, total energy demand will increase in all locations when

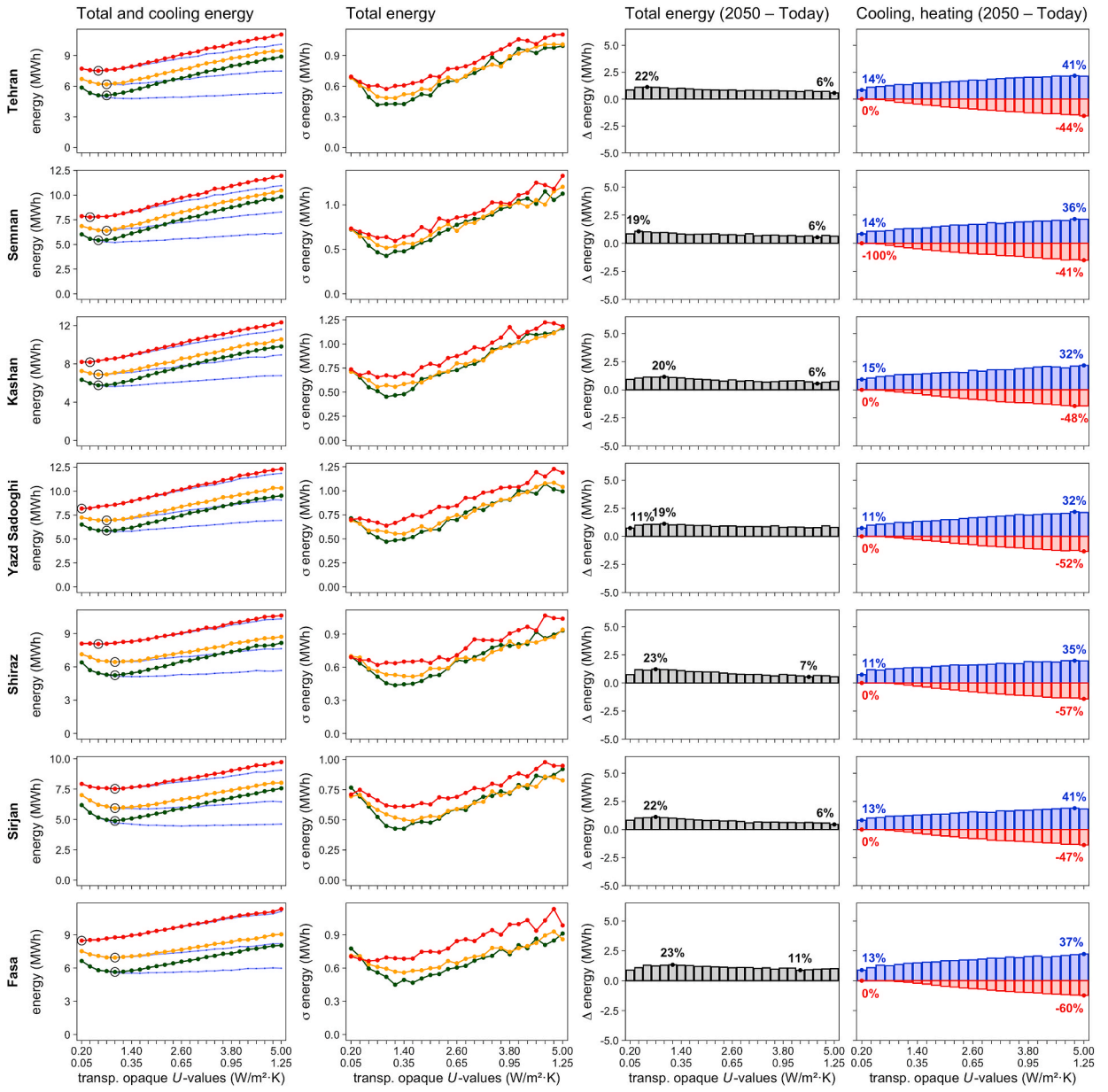

Fig. 6. Group 2 – Comparison between present-day (green lines), 2050 (orange), and 2080 (red) timeframes. Graphs in the first column depict the average total energy needs – blue lines illustrate the cooling energy needs, and black circles indicate the ideal pair of *U*-values for each timeframe. The second column presents the standard deviation (σ). The third and fourth columns present the difference in total energy needs (Δ) and cooling (blue bars) and heating (red bars) energy needs (Δ) between the 2050 and present-day timeframes. (For interpretation of the references to colour in this figure legend, the reader is referred to the Web version of this article.)

comparing 2050 to the present-day climate (up to 13% for buildings with low *U*-values and up to 38% for those with high *U*-values). This result is in line with the findings of Roshan, Arab et al. [24], which confirm an increase in total energy demand for residential buildings in Bandar Abbas, Bushehr, and Chabahar. It also predicts a decrease in thermal comfort days for the next decades as temperature and moisture content increase.

Due to the high temperatures of the outdoor environment, the energy demand for air conditioning in Group 3 buildings is higher than in the other groups. Therefore, buildings in all locations of this group require the smallest possible *U*-values in present-day and future climates to reduce the heat gains through the envelope—in this study, the lowest values were 0.05 W m^{-2} K^{-1} and 0.20 W m^{-2} K^{-1} for opaque and transparent elements, respectively. As shown in Table 3, all these locations have an average temperature above the cooling setpoint (25 °C) for today and future timeframes, daily minimum average temperatures near or above the heating setpoint (20 °C), and daily maximum average temperatures reaching 38 °C.

As for the effect of the building geometry, different trends were recognized from the standard deviation comparisons (graphs in the

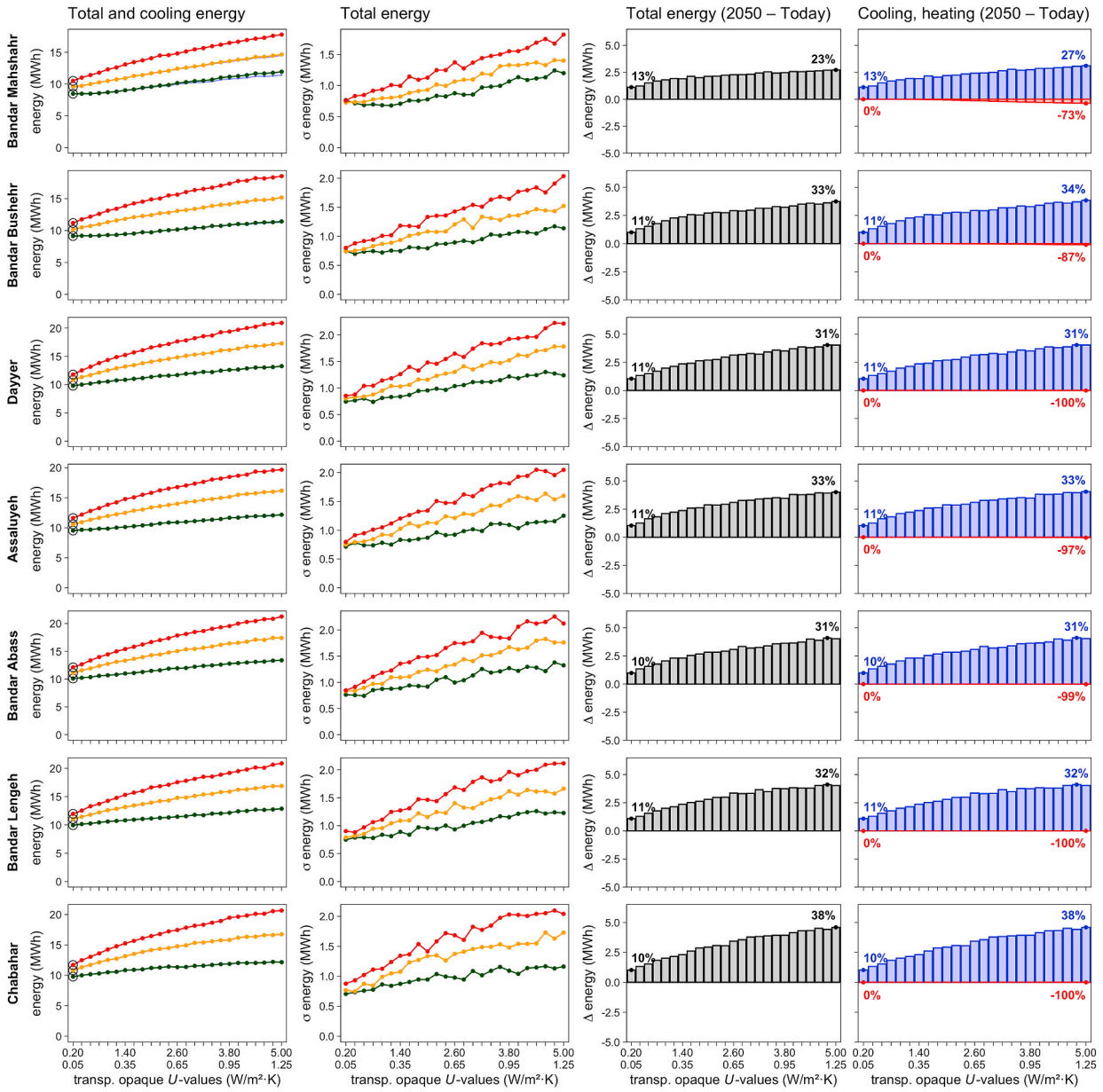

Fig. 7. Group 3 – Comparison between present-day (green lines), 2050 (orange), and 2080 (red) timeframes. Graphs in the first column depict the average total energy needs – blue lines illustrate cooling energy needs, and black circles indicate the ideal pair of *U*-values for each timeframe. The second column presents the standard deviation (σ). The third and fourth columns present the difference in total energy needs (Δ) and cooling (blue bars) and heating (red bars) energy needs (Δ) between the 2050 and present-day timeframes. (For interpretation of the references to colour in this figure legend, the reader is referred to the Web version of this article.)

second column in Figs. 5, Figure 6, and Fig. 7). In Groups 1 and 2, geometry tends to have a greater impact on buildings with very low or high *U*-values, thus producing a higher variation in energy performance than in the ideal *U*-values range. Furthermore, in both groups, values demonstrate that building geometry will have a similar or slightly greater impact in the future, particularly in 2080. For Group 3, however, global warming and the increase in *U*-values clearly show that geometry has a greater influence on the energy performance of buildings.

The results from this study demonstrate that global warming will significantly increase cooling needs in Iran. It also shows that, generally, present-day ideal *U*-values will not be the ideal *U*-values in the future, ultimately leading to overheating. Overall, as latitude lowers toward hotter regions (Group 1 to Group 3), the trend is to reduce thermal transmittance values. , The ideal *U*-values tend to increase for cities in Group 1, to be lower in Group 2, and to be the lowest possible in Group 3. Table 6 summarizes these trends. These findings also show that the design of future buildings must consider each location's specificity and the impact of climate change in each specific region of Iran.

Table 4
Group 1 – Overheating from present-day ideal *U*-values in future timeframes (impact greater or equal to 3% are marked in bold).

Location	Present-day	2050				2080			
	Ideal *U*-values[a]	Energy (MW·h)	Impact of present-day ideal *U*-values			Energy (MW·h)	Impact of present-day ideal *U*-values		
			Δ *U*-values[a] ($W \cdot m^{-2} \cdot K^{-1}$)	Δ energy (MW·h)	(%)		Δ *U*-values[a] ($W \cdot m^{-2} \cdot K^{-1}$)	Δ energy (MW·h)	(%)
Tabriz	0.15/0.6	4.86 ± 0.52	0.05/0.2	0.03 ± 0.03	0.7	6.01 ± 0.57	0.10/0.4	0.16 ± 0.03	2.8
Rasht (coastal)	0.20/0.8	5.41 ± 0.36	0.05/0.2	0.05 ± 0.03	0.8	6.66 ± 0.47	0.05/0.2	0.07 ± 0.03	1.0
Ramsar (coastal)	0.20/0.8	5.65 ± 0.41	0.05/0.2	0.08 ± 0.03	1.4	6.97 ± 0.52	0.05/0.2	0.06 ± 0.03	0.9
Nowshahr (coastal)	0.25/1.0	5.46 ± 0.40	0.05/0.2	0.06 ± 0.03	1.0	6.79 ± 0.47	0.05/0.2	0.05 ± 0.03	0.7
Sari (coastal)	0.20/0.8	5.81 ± 0.45	0.05/0.2	0.01 ± 0.03	0.1	7.08 ± 0.52	0.05/0.2	0.06 ± 0.03	0.9
Karaj	0.15/0.6	4.68 ± 0.52	0.10/0.4	0.18 ± 0.03	**4.0**	5.79 ± 0.57	0.10/0.4	0.21 ± 0.06	**3.8**
Hamedan	0.15/0.6	4.47 ± 0.52	0.10/0.4	0.25 ± 0.03	**5.9**	5.57 ± 0.59	0.15/0.6	0.39 ± 0.03	**7.6**

[a] Opaque and transparent elements, respectively.

In conclusion, Iran will be particularly affected by global warming, with a severe impact on the energy performance of buildings. Climate change will lead buildings to underperform if thermal transmittance is only optimized for the present-day climate. However, the trend of the ideal thermal transmittance values varies according to each climate region in Iran. Current locations with low to high heating needs will have higher ideal *U*-values in a warmer future. However, for those locations where buildings already have high cooling needs, the trends will be to have lower or the lowest possible *U*-values.

As mentioned in the introduction, only two studies have compared the performance of optimized buildings in the current climate and future climate conditions in Iran. The first study analyzed an educational building [27] and the second a residential building [28], both in Tehran, and their conclusions are in line with the findings of this study—optimized solutions will no longer be ideal in the future, despite contributing to reducing energy consumption when compared to the base case without optimization. Another study that identified the ideal thermal transmittance in a different Middle East country shows a significant reduction in total energy in the future when compared to a building without optimization in current climate conditions [15]. Nonetheless, both studies reveal the importance of optimizing buildings for current climate conditions. Even if the optimization is less effective in the future, it places their energy performance near optimum values. Nevertheless, this will not be enough to face the challenges posed by climate change. If a nation aims to be carbon neutral and prevent the building stock from being locked into sub-optimal solutions, edifices must be designed to consider the evolving regional climate during the entire lifespan of the buildings.

Therefore, the approach to mitigate climate change should differ depending on the trend of the ideal *U*-values. When the trend is to raise the ideal *U*-values (Group 1), the buildings should be designed to balance current and future ideal *U*-values from the start, as downgrading the building will be particularly difficult and costly, with significant construction waste-related impacts. In the cases where the trend is to have lower values in the future (Group 2), buildings should be designed and built to consider current climate conditions and be retrofitted as the climate evolves. Although it may turn out more costly in the long run than designing a building that already considers future climate conditions, this is a cautious approach that factors in the uncertainty associated with climate change.

For example, consider the same single-family house in Karaj and Kashan, both having a common double-brick wall construction with an interior insulation layer. Both locations require the same present-day ideal *U*-value of 0.15 $W\,m^{-2}\,K^{-1}$ for the opaque elements, which corresponds to a wall insulation thickness of 19 cm. In the case of Karaj (Group 1), the ideal *U*-value for 2080 will increase to 0.25 $W\,m^{-2}\,K^{-1}$, thus reducing the thickness to 9 cm. However, in the case of Kashan (Group 2), the future ideal *U*-value will decrease to 0.1 $W\,m^{-2}\,K^{-1}$, meaning an increase to 33 cm in thickness. Therefore, in the first case, the building should already consider the future climate, as retrofitting would require demolishing the walls to partially remove the insulation. In the second case, as the building can be easily retrofitted by adding one extra insulation layer on the outside face of the exterior wall, optimizing the building for current climate conditions is recommended.

These mitigation strategies make even more sense if one considers that there is no linear correspondence between the thermal transmittance step and the thicknesses of the elements. This signifies that the thicknesses will increase dramatically as the lower segment of the *U*-values range is reached, while in the upper segment, the thicknesses tend to be smaller. In the case when the ideal *U*-values must be the lowest possible for today's climate (Group 3), the strategy should be to consider a cost-benefit construction. This difference in design strategy is dramatically important, as this study demonstrates there is no single guideline to counterbalance the effects of climate change, but rather different guidelines, each one specific to its region and the local effects of climate change. Therefore, further research that analyzes different building types and regional climates is required. In addition, building professionals and policymakers need to consider this in designing optimal buildings and implementing legislation that contemplates contrasting climates within a country's territory.

This study has a few limitations that must be mentioned. First, Iran has several climate regions with distinguishable cultural, social,

Table 5
Group 2 – Overheating from present-day ideal *U*-values in future timeframes (impacts greater or equal to 3% are marked in bold).

Location	Present-day	2050				2080			
	Ideal *U*-values[a]	Energy (MW·h)	Impact of present-day ideal *U*-values			Energy (MW·h)	Impact of present-day ideal *U*-values		
			Δ *U*-values[a] ($W \cdot m^{-2} \cdot K^{-1}$)	Δ energy (MW·h)	(%)		Δ *U*-values[a] ($W \cdot m^{-2} \cdot K^{-1}$)	Δ energy (MW·h)	(%)
Tehran	0.20/0.8	6.19 ± 0.50	–	0 ± 0.03	–	7.58 ± 0.61	−0.05/−0.2	0.07 ± 0.04	0.9
Semnan	0.15/0.6	6.39 ± 0.63	0.05/0.2	0.04 ± 0.04	0.7	7.82 ± 0.67	−0.05/−0.2	0.05 ± 0.04	0.6
Kashan	0.15/0.6	6.89 ± 0.62	–	0 ± 0.04	–	8.33 ± 0.70	−0.05/−0.2	0.14 ± 0.04	1.8
Yazd Sadooghi	0.20/0.8	6.94 ± 0.59	–	0 ± 0.04	–	8.48 ± 0.67	−0.15/−0.6	0.30 ± 0.04	**3.7**
Shiraz	0.25/1.0	6.43 ± 0.53	–	0 ± 0.04	–	8.15 ± 0.64	−0.10/−0.4	0.09 ± 0.04	1.2
Sirjan	0.25/1.0	5.93 ± 0.55	–	0 ± 0.04	–	7.53 ± 0.61	–	0 ± 0.04	–
Fasa	0.25/1.0	6.94 ± 0.59	–	0 ± 0.04	–	8.77 ± 0.70	−0.20/−0.8	0.29 ± 0.05	**3.5**

[a] Opaque and transparent elements, respectively.

Table 6
Trend of ideal *U*-values in each group and timeframe using present-day climate as reference.

Group 1	Higher	Higher
Group 2	Equal	Lower
Group 3	Lowest	Lowest
	2050	**2080**
	Timeframe	

and technological characteristics. The functional program and the operation specifications were designed to consider the well-known needs of a single family, but this "average" profile does not consider these different characteristics in its analysis. For example, the heating and cooling setpoints may vary between regions, there may be different shadowing elements to protect glazing areas from solar radiation, or there may even be other rooms with different sizes that fit a family's way of life. Second, although the study covers many locations, these in no way cover all the possible cases in Iran. This, in turn, may provide an incomplete view of the country. Third, this study does not cover all climate change scenarios, as the SSP5-8.5 is only one of the IPCC's scenarios. Other scenarios may prove more probable if the countries' carbon emissions and other greenhouse gases are reduced. In those cases, the simulation of future buildings must consider improvements in the energy efficiency of equipment, production of renewable energy, and increase in electric energy use. Fourth, the solar heat gain coefficient may also vary according to the window *U*-value. Still, it should be noted that the results are discussed mainly based on the comparison between the present and future, mitigating the effects of the uncertainty of these parameters. Lastly, projections from different climate models may diverge significantly. In this sense, this study only provides a snapshot of what might be probable; thus, complementary studies are needed.

4. Conclusions

This study deepens our understanding of how one of the climate change scenarios will impact present-day buildings with ideal thermal transmittances and how these will evolve over the 21st century in the Iranian territory. Additionally, the study utilizes a unique approach to generate thousands of single-family buildings and morphs today's typical meteorological year data to match the SSP5-8.5 scenario using the novel Future Weather Generator. Due to the large number of buildings simulated, this work has the advantage of being statistically significant, thus allowing higher confidence in generalizing results than studies that use a single or a small number of archetypes.

The main contributions to the body of knowledge can be summarized as follows:

- Global warming will severely affect the performance of residential buildings in Iran. However, the impact varies according to each climate region. For example, residential buildings located on the coast of the Caspian Sea will have the lowest relative increase in total energy demand. Conversely, as the latitude decreases, buildings with medium (located in the central plateau of Iran) or low (located on the coast of the Persian Gulf) heating needs will increase total energy needs. Also, in locations with a high need for cooling (located on the coast of the Persian Gulf), buildings will require substantially higher energy to cool down, as a warmer future exacerbates their already high cooling demand.
- In the interior northwest of Iran, the impact of climate change will differ according to the thermal transmittance of the building envelope. For instance, buildings with high *U*-values have higher total energy demand today than in the future. Conversely, buildings with very low *U*-values will have higher energy needs in the future, mainly due to cooling needs.
- The results also show that today's ideal *U*-values will differ from future ones depending on the climate region. In some locations, present-day ideal *U*-values will increase total energy demand by up to 8% compared to future ideal *U*-values.
- The trend of ideal *U*-values from the present day to 2080 can be grouped into three regions. In the first group, ideal *U*-values tend to increase, meaning that buildings will need to be downgraded in the future to continue to have optimal performance. In the second group, the future ideal *U*-values will be lower than today's; thus, current buildings may need to be retrofitted as the climate gets warmer. Lastly, buildings on the coast of the Persian Gulf must have the lowest possible thermal transmittances, as the outdoor conditions are already too stringent and will become even worse in the future.
- Lastly, as not all locations will be affected equally by global warming, each region will require specific design decisions. Professionals must consider future climate projections and seek a design strategy for the whole life span of the building. This effort will lead to an increased effort by design professionals, particularly skills to deal with uncertainty related to future uses, systems operation, and equipment efficiency, among other aspects. Lastly, policymakers should consider implementing a building code that considers climate change and the potential effects this may have on the buildings' energy performance.

The findings should not be generalized to all types of residential buildings, as this study only covers single-family houses. In this sense, future work should analyze other types, such as multi-story apartment buildings, which are the most common in Iran, as the methodology may be extended to include them. Other applications of this methodology may be to analyze the impact of climate change in different world regions or to analyze other envelope thermophysical properties.

CRediT author Statement

Eugénio Rodrigues: Conceptualization, Methodology, Software, Investigation, Data Curation, Formal Analysis, Visualization, Writing - Original Draft, Writing - Review & Editing, Project Administration, Funding Acquisition, Supervision; **Nazanin Azimi Fereidani:** Conceptualization, Investigation, Formal Analysis, Writing – Original Draft, Writing – Review & Editing; **Marco S. Fernandes:** Conceptualization, Software, Investigation, Writing - Review & Editing; **Adélio R. Gaspar:** Conceptualization, Writing - Review & Editing, Supervision, Resources.

Declaration of competing interest

The authors declare that they have no known competing financial interests or personal relationships that could have appeared to influence the work reported in this paper.

Data availability

The dataset of the experiment is available at the URL: https://doi.org/10.6084/m9.figshare.21905682.

Acknowledgments

The presented work is framed under the *Energy for Sustainability Initiative* of the University of Coimbra (UC).

We acknowledge the World Climate Research Programme, which through its Working Group on Coupled Modelling, coordinated and promoted CMIP6. In addition, we thank the climate modeling groups for producing and making their model output available, the Earth System Grid Federation (ESGF) for archiving and providing access to the data, and the multiple funding agencies that support CMIP6 and ESGF.

The Portuguese Foundation for Science and Technology (FCT) supported this work [grant number PTDC/EME-REN/3460/2021]. In addition, FCT supports Eugénio Rodrigues and Marco S. Fernandes through researcher contracts [2021.00230. CEECIND and 2021.02975. CEECIND, respectively], and Nazanin Azimi Fereidani through a Ph.D. fellowship [SFRH/BD/151355/2021].

The authors are grateful to Anabela Reis Alves for proofreading the manuscript.

References

[1] S. Mohammad, A. Shea, Performance evaluation of modern building thermal envelope designs in the semi-arid continental climate of tehran, Buildings 3 (2013) 674–688, https://doi.org/10.3390/buildings3040674.
[2] D. Ürge-Vorsatz, R. Khosla, R. Bernhardt, Y.C. Chan, D. Vérez, S. Hu, L.F. Cabeza, Advances toward a net-zero global building sector, Annu. Rev. Environ. Resour. 45 (2020) 227–269, https://doi.org/10.1146/annurev-environ-012420-045843.
[3] N. Azimi Fereidani, E. Rodrigues, A.R. Gaspar, A review of the energy implications of passive building design and active measures under climate change in the Middle East, J. Clean. Prod. 305 (2021), 127152, https://doi.org/10.1016/j.jclepro.2021.127152.
[4] D. D'Agostino, F. de' Rossi, M. Marigliano, C. Marino, F. Minichiello, Evaluation of the optimal thermal insulation thickness for an office building in different climates by means of the basic and modified "cost-optimal" methodology, J. Build. Eng. 24 (2019), 100743, https://doi.org/10.1016/j.jobe.2019.100743.
[5] M. Vellei, A.P. Ramallo-González, D. Coley, J. Lee, E. Gabe-Thomas, T. Lovett, S. Natarajan, Overheating in vulnerable and non-vulnerable households, Build. Res. Inf. 45 (2017) 102–118, https://doi.org/10.1080/09613218.2016.1222190.
[6] D. Chen, Overheating in residential buildings: challenges and opportunities, Indoor Built Environ. 28 (2019) 1303–1306, https://doi.org/10.1177/1420326X19871717.
[7] E. Rodrigues, M.S. Fernandes, Overheating risk in Mediterranean residential buildings: comparison of current and future climate scenarios, Appl. Energy 259 (2020), 114110, https://doi.org/10.1016/j.apenergy.2019.114110.
[8] L. Pajek, M. Jevrić, I. Ćipranić, M. Košir, A multi-aspect approach to energy retrofitting under global warming: a case of a multi-apartment building in Montenegro, J. Build. Eng. 63 (2023), 105462, https://doi.org/10.1016/j.jobe.2022.105462.
[9] F. Ascione, R.F. De Masi, A. Gigante, G.P. Vanoli, Resilience to the climate change of nearly zero energy-building designed according to the EPBD recast: monitoring, calibrated energy models and perspective simulations of a Mediterranean nZEB living lab, Energy Build. 262 (2022), 112004, https://doi.org/10.1016/j.enbuild.2022.112004.
[10] C. Baglivo, P.M. Congedo, G. Murrone, D. Lezzi, Long-term predictive energy analysis of a high-performance building in a mediterranean climate under climate change, Inside Energy 238 (2022), 121641, https://doi.org/10.1016/j.energy.2021.121641.
[11] Y. Kharbouch, M. Ameur, Prediction of the impact of climate change on the thermal performance of walls and roof in Morocco, Int. Rev. Appl. Sci. Eng. 13 (2022) 174–184, https://doi.org/10.1556/1848.2021.00330.
[12] K. Bamdad, M.E. Cholette, S. Omrani, J. Bell, Future energy-optimised buildings — addressing the impact of climate change on buildings, Energy Build. 231 (2021), 110610, https://doi.org/10.1016/j.enbuild.2020.110610.
[13] M. Karimpour, M. Belusko, K. Xing, J. Boland, F. Bruno, Impact of climate change on the design of energy efficient residential building envelopes, Energy Build. 87 (2015) 142–154, https://doi.org/10.1016/j.enbuild.2014.10.064.
[14] K. Verichev, M. Zamorano, A. Fuentes-Sepúlveda, N. Cárdenas, M. Carpio, Adaptation and mitigation to climate change of envelope wall thermal insulation of residential buildings in a temperate oceanic climate, Energy Build. 235 (2021), 110719, https://doi.org/10.1016/j.enbuild.2021.110719.
[15] H. Radhi, Evaluating the potential impact of global warming on the UAE residential buildings – a contribution to reduce the CO2 emissions, Build. Environ. 44 (2009) 2451–2462, https://doi.org/10.1016/j.buildenv.2009.04.006.
[16] B. Rosti, A. Omidvar, N. Monghasemi, Optimal insulation thickness of common classic and modern exterior walls in different climate zones of Iran, J. Build. Eng. 27 (2020), 100954, https://doi.org/10.1016/j.jobe.2019.100954.
[17] K. Aliakbari, A. Ebrahimi-Moghadam, P. Ildarabadi, Investigating the impact of a novel transparent nano-insulation in building windows on thermal comfort conditions and energy consumptions in different climates of Iran, Therm. Sci. Eng. Prog. 25 (2021), 101009, https://doi.org/10.1016/j.tsep.2021.101009.
[18] F. Yousefi, Y. Gholipour, Y. Saboohi, W. Yan, Interaction of glazing parameters, climatic condition and interior shadings: performing energy and cost analysis in a residential building in Iran, Energy Effic 13 (2020) 159–176, https://doi.org/10.1007/s12053-019-09831-w.
[19] N. Delgarm, B. Sajadi, K. Azarbad, S. Delgarm, Sensitivity analysis of building energy performance: a simulation-based approach using OFAT and variance-based sensitivity analysis methods, J. Build. Eng. 15 (2018) 181–193, https://doi.org/10.1016/j.jobe.2017.11.020.
[20] M. Tavakolan, F. Mostafazadeh, S. Jalilzadeh Eirdmousa, A. Safari, K. Mirzaei, A parallel computing simulation-based multi-objective optimization framework for economic analysis of building energy retrofit: a case study in Iran, J. Build. Eng. 45 (2022), 103485, https://doi.org/10.1016/j.jobe.2021.103485.

[21] G. Roshan, J. Orosa, T. Nasrabadi, Simulation of climate change impact on energy consumption in buildings, case study of Iran, Energy Pol. 49 (2012) 731–739, https://doi.org/10.1016/j.enpol.2012.07.020.
[22] G. Roshan, A. Ghanghermeh, J.A. Orosa, Thermal comfort and forecast of energy consumption in Northwest Iran, Arabian J. Geosci. 7 (2014) 3657–3674, https://doi.org/10.1007/s12517-013-0973-7.
[23] G. Roshan, J.A. Orsa, Regional climate changes and their effects on monthly energy consumption in buildings in Iran, Nat. Environ. Chang. 1 (2015) 31–48. https://jnec.ut.ac.ir/article_55069.html.
[24] G. Roshan, M. Arab, V. Klimenko, Modeling the impact of climate change on energy consumption and carbon dioxide emissions of buildings in Iran, J. Environ. Heal. Sci. Eng. 17 (2019) 889–906, https://doi.org/10.1007/s40201-019-00406-6.
[25] G. Roshan, R. Oji, S. Attia, Projecting the impact of climate change on design recommendations for residential buildings in Iran, Build. Environ. 155 (2019) 283–297, https://doi.org/10.1016/j.buildenv.2019.03.053.
[26] G. Roshan, M. Moghbel, M. Farrokhzad, Mitigation of climate change impact using green wall and green roof strategies: comparison between two different climate regions in Iran, Theor. Appl. Climatol. 150 (2022) 167–184, https://doi.org/10.1007/s00704-022-04146-w.
[27] K. Aram, R. Taherkhani, A. Šimelytė, Multistage optimization toward a nearly net zero energy building due to climate change, Energies 15 (2022) 983, https://doi.org/10.3390/en15030983.
[28] F. Mostafazadeh, S.J. Eirdmousa, M. Tavakolan, Energy, economic and comfort optimization of building retrofits considering climate change: a simulation-based NSGA-III approach, Energy Build. 280 (2023), 112721, https://doi.org/10.1016/j.enbuild.2022.112721.
[29] H.E. Beck, N.E. Zimmermann, T.R. McVicar, N. Vergopolan, A. Berg, E.F. Wood, Present and future Köppen-Geiger climate classification maps at 1-km resolution, Sci. Data 5 (2018), 180214, https://doi.org/10.6084/m9.figshare.6396959.
[30] E. Rodrigues, M.S. Fernandes, D. Carvalho, Future weather generator for building performance research: an open-source morphing tool and an application, Build. Environ. 233 (2023), 110104, https://doi.org/10.1016/j.buildenv.2023.110104.
[31] R. Döscher, M. Acosta, A. Alessandri, P. Anthoni, T. Arsouze, T. Bergman, R. Bernardello, S. Boussetta, L.-P. Caron, G. Carver, M. Castrillo, F. Catalano, I. Cvijanovic, P. Davini, E. Dekker, F.J. Doblas-Reyes, D. Docquier, P. Echevarria, U. Fladrich, R. Fuentes-Franco, M. Gröger, J.v. Hardenberg, J. Hieronymus, M. P. Karami, J.-P. Keskinen, T. Koenigk, R. Makkonen, F. Massonnet, M. Ménégoz, P.A. Miller, E. Moreno-Chamarro, L. Nieradzik, T. van Noije, P. Nolan, D. O'Donnell, P. Ollinaho, G. van den Oord, P. Ortega, O.T. Prims, A. Ramos, T. Reerink, C. Rousset, Y. Ruprich-Robert, P. Le Sager, T. Schmith, R. Schrödner, F. Serva, V. Sicardi, M. Sloth Madsen, B. Smith, T. Tian, E. Tourigny, P. Uotila, M. Vancoppenolle, S. Wang, D. Wårlind, U. Willén, K. Wyser, S. Yang, X. Yepes-Arbós, Q. Zhang, The EC-earth3 earth system model for the coupled model intercomparison project 6, Geosci. Model Dev. (GMD) 15 (2022) 2973–3020, https://doi.org/10.5194/gmd-15-2973-2022.
[32] W. Hazeleger, X. Wang, C. Severijns, S. Ştefănescu, R. Bintanja, A. Sterl, K. Wyser, T. Semmler, S. Yang, B. van den Hurk, T. van Noije, E. van der Linden, K. van der Wiel, EC-Earth V2.2: description and validation of a new seamless earth system prediction model, Clim. Dynam. 39 (2012) 2611–2629, https://doi.org/10.1007/s00382-011-1228-5.
[33] R. Haarsma, M. Acosta, R. Bakhshi, P.-A. Bretonnière, L.-P. Caron, M. Castrillo, S. Corti, P. Davini, E. Exarchou, F. Fabiano, U. Fladrich, R. Fuentes Franco, J. García-Serrano, J. von Hardenberg, T. Koenigk, X. Levine, V.L. Meccia, T. van Noije, G. van den Oord, F.M. Palmeiro, M. Rodrigo, Y. Ruprich-Robert, P. Le Sager, E. Tourigny, S. Wang, M. van Weele, K. Wyser, HighResMIP versions of EC-Earth: EC-Earth3P and EC-Earth3P-HR – description, model computational performance and basic validation, Geosci. Model Dev. (GMD) 13 (2020) 3507–3527, https://doi.org/10.5194/gmd-13-3507-2020.
[34] B.C. O'Neill, C. Tebaldi, D.P. van Vuuren, V. Eyring, P. Friedlingstein, G. Hurtt, R. Knutti, E. Kriegler, J.-F. Lamarque, J. Lowe, G.A. Meehl, R. Moss, K. Riahi, B. M. Sanderson, The scenario model intercomparison project (ScenarioMIP) for CMIP6, geosci, Model Dev 9 (2016) 3461–3482, https://doi.org/10.5194/gmd-9-3461-2016.
[35] E. Rodrigues, M.S. Fernandes, D. Carvalho, M.S. Fernandes, Documentation of future weather generator. https://adai.pt/future-weather-generator/documentation/, 2022. (Accessed 30 March 2022).
[36] E. Rodrigues, M.S. Fernandes, Á. Gomes, A.R. Gaspar, J.J. Costa, Performance-based design of multi-story buildings for a sustainable urban environment: a case study, Renew. Sustain. Energy Rev. 113 (2019), 109243, https://doi.org/10.1016/j.rser.2019.109243.
[37] E. Rodrigues, A.R. Gaspar, Á. Gomes, An evolutionary strategy enhanced with a local search technique for the space allocation problem in architecture, Part 1: methodology, Comput. Des. 45 (2013) 887–897, https://doi.org/10.1016/j.cad.2013.01.001.
[38] E. Rodrigues, A.R. Gaspar, Á. Gomes, An approach to the multi-level space allocation problem in architecture using a hybrid evolutionary technique, Autom. ConStruct. 35 (2013) 482–498, https://doi.org/10.1016/j.autcon.2013.06.005.
[39] E. Rodrigues, A.R. Gaspar, Á. Gomes, An evolutionary strategy enhanced with a local search technique for the space allocation problem in architecture, Part 2: validation and performance tests, Comput. Des. 45 (2013) 898–910, https://doi.org/10.1016/j.cad.2013.01.003.
[40] E. Rodrigues, A.R. Gaspar, Á. Gomes, Automated approach for design generation and thermal assessment of alternative floor plans, Energy Build. 81 (2014) 170–181, https://doi.org/10.1016/j.enbuild.2014.06.016.
[41] Climate OneBuilding, Org – repository of free climate data for building performance simulation. http://climate.onebuilding.org/default.html, 2021. (Accessed 27 May 2021).
[42] Department of Housing and Urban Development, National Building Regulations of Iran, fourth ed., Building and Housing Research Center, Tehran, 2019.